

An Epidemiological Modeling Take on Religion Dynamics

Bilge Taskin^{1,x}, Teddy Lazebnik^{1,2,x,*}

¹ Department of Computing, Jonkonping University, Jonkoping, Sweden

² Department of Information Systems, University of Haifa, Haifa, Israel

^x These authors contributed equally.

* Corresponding author: teddy.lazebnik@ju.se

Abstract

Religions are among the most consequential social institutions, shaping collective identities, moral norms, and political organization across societies and historical periods. Nevertheless, despite extensive scholarship describing conversion, competition, and secularization, there is still no widely adopted formal model that captures religious dynamics over time within a unified, mechanistic framework. In this study, we propose an epidemiologically grounded model of religious change in which religions spread and compete analogously to co-circulating strains. The model extends multi-strain compartmental dynamics by distinguishing passive believers, active missionaries, and religious elites, and by incorporating demographic turnover and mutation-like splitting that endogenously generates new denominations. Using computer simulations, we show that the same mechanism reproduces canonical qualitative regimes, including emergence from rarity, rapid expansion, long-run coexistence, and transient rise-and-fall movements. A reduced calibration variant fits historical affiliation trajectories with parsimonious regime shifts in effective recruitment and disaffiliation, yielding interpretable signatures of changing social conditions. Finally, sensitivity analyses map sharp regime boundaries in parameter space, indicating that modest shifts in recruitment efficacy or retention among active spreaders can qualitatively alter long-run religious landscapes. These results establish a general, interpretable framework for studying religion as a dynamical diffusion process and provide a tool for comparative inference and counterfactual analysis in sociological research.

Keywords: religious dynamics, multi-strain contagion; mathematical sociology; digital humanities; SIR model.

1 Introduction

Religion has played a central role in shaping human societies, influencing cultural identity, political institutions, and collective behavior throughout history [1, 2, 3]. In early agricultural societies, animistic and polytheistic traditions provided explanatory frameworks for natural phenomena and mechanisms for social cohesion [4, 5, 6]. The institutionalization of priesthoods and ritual practices in Mesopotamia, Egypt, and the Indus Valley can be seen as early examples of religion serving as a stabilizing force for centralized states, legitimizing political authority and codifying moral order [7, 8, 9]. Later, the emergence of axial-age religions such as Judaism, Buddhism, Confucianism, and early Greek philosophy introduced universal moral codes and abstract cosmologies, enabling broader social integration and the consolidation of empires [10, 11, 12]. Following this in the historical record, in the classical and medieval periods, the spread of Christianity and Islam illustrates how religious movements can transcend ethnic and geographic boundaries, often accompanying processes of imperial expansion, trade, and conquest [13, 14, 15]. Religious institutions became central to governance, education, and law, shaping not only the political order but also economic practices such as taxation, charity, and land distribution [16, 17]. Nowadays,

modernity has not diminished religion's influence, but transformed its modalities of spread and competition. The Enlightenment and secularization movements challenged traditional institutions, yet religion adapted by giving rise to new denominations, evangelical movements, and, in some cases, politically mobilized fundamentalisms [18, 19, 20]. In the globalized era, religions circulate alongside cultural products and ideas, facilitated by digital media and migration [21, 22]. Contemporary dynamics include the rapid rise of Pentecostalism in the Global South, the global networking of Islam, and the proliferation of new religious movements and cults [23, 24, 25]. At the same time, disaffiliation and secular humanism have emerged as significant counter-trends in many industrialized societies [26].

These historical patterns strongly suggest that religions function analogously to evolving systems of ideas that compete for adherents and adapt to shifting socio-political environments [27]. Crucially, religion not only spreads within societies but also reshapes them, influencing demographic patterns, institutional stability, and economic organization [28]. For this reason, the spread of religion has long been a subject of scholarly attention across disciplines [29, 30, 31, 32]. Historians and sociologists have examined large-scale processes of conversion, conflict, and reform; anthropologists have investigated the ritual, symbolic, and cultural mechanisms that facilitate belief transmission; and political scientists have studied the role of religion in shaping governance, legitimacy, and social movements.

Despite this wealth of scholarship, formal dynamic models of religious spread remain comparatively underdeveloped [33]. Traditional analyses often describe correlations or provide historical narratives but rarely capture the feedback loops and temporal patterns through which religions expand, compete, or decline. To address this limitation, recent research has drawn attention to the structural similarities between the spread of religions and the spread of infectious diseases [34, 35]. Both involve populations of susceptible individuals, mechanisms of contact that facilitate transmission, processes of “infection” (conversion), and “recovery” (disaffiliation or apostasy). Furthermore, just as pathogens may coexist, compete, or mutate, so too can religions diversify, fragment, and evolve.

This analogy naturally motivates the application of epidemiological models, particularly the Susceptible–Infected–Recovered (SIR) framework [36] to the study of religion. To this end, in this work, we introduce a multi-strain SIR model for religious dynamics in which each religion is modeled as a distinct strain and the effective transmission rate is defined as a function of social and political properties. By explicitly integrating contextual variables into the epidemiological framework, our model accounts for both rapid bursts of religious expansion and long-term coexistence of competing belief systems. We further demonstrate how this approach can replicate historical patterns such as the sudden rise of new religions, the splitting of established faiths, and cyclical revival movements.

This paper makes three primary contributions. First, we present a formal model that generalizes classical epidemiological approaches to capture the complexity of religious dynamics. Second, we propose methods for linking model parameters with empirical socio-political data. Third, we validate the model through experiments that reproduce known historical cases, thereby demonstrating its explanatory and predictive potential. Taken together, our results provide a rigorous framework for studying religion as a dynamic, contagious process shaped by the interplay between belief systems and their broader social environments.

The remainder of this paper is organized as follows. Section 2 reviews mathematical models of cultural and religious diffusion, as well as epidemiological approaches to idea transmission. Section 3 formally introduces our multi-strain SIR model, including the formal definitions of states, transitions, and the socio-political dependence of the transmission parameter. Section 4.1 details our empirical methodology, covering data collection, parameter

fitting, and experimental design. Section 4.2 outlines the obtained findings, focusing on the emergence of new religions, the splitting of established traditions, the rise-and-fall cycles of cults, and the model's fit to historical records. Finally, Section 5 discusses the applicative outcomes of the study, its limitations, and directions for future research.

2 Related Work

In this section, we review the underlying religion spread dynamics that one should consider in any modeling effort, followed by a short review of epidemiological modeling practices with a focus on extended SIR models with multi-strain.

2.1 Religion spread dynamics

Religion has long been recognized as one of the most enduring and influential forces in human societies [37, 38, 39]. It provides not only systems of belief but also shared practices, moral codes, and institutional structures that bind communities together and regulate social behavior [40]. Scholars across sociology, anthropology, history, and political science have examined religion as both a driver and a product of social change, noting its capacity to shape collective identities, stabilize political orders, and motivate large-scale cooperation [41, 42, 43, 44]. At the same time, religion has been a source of competition, division, and conflict, often catalyzing transformative cultural and political shifts [45, 46].

The spread of religion is not simply a matter of individual belief but a complex socio-cultural process influenced by institutions, social networks, and political environments. Early anthropological theories emphasized religion as a form of “social glue”, binding communities through ritual and shared narratives [47]. In agricultural and early state societies, religious practices often reinforced stratified political hierarchies: priesthoods legitimized rulers, while rulers endowed temples, intertwining spiritual authority with political power [48]. The integration of religion into law and governance provided durable mechanisms for transmitting norms across generations and stabilizing expanding polities [49].

At a macro-historical scale, religion often spread through contact processes that resemble contagion: through trade, conquest, migration, and missionary activity [50]. The expansion of Buddhism along the Silk Road, Christianity throughout the Roman Empire, and Islam across North Africa and into Asia are notable examples where the growth of religious communities followed routes of human mobility and exchange [51, 52]. In such contexts, social prestige, institutional support, and political patronage frequently amplified the rate of conversion, while persecution and legal restrictions could slow or suppress diffusion. Thus, the likelihood of religious adoption was never purely a matter of theology but deeply conditioned by social and political context [53].

Another key feature of religious spread is competition among belief systems. Rarely do religions exist in isolation; instead, they compete for adherents within overlapping populations. This competition can manifest as coexistence (as in multi-religious empires), dominance by a single tradition (as in state religions), or dynamic cycles of conversion and reform. Religious competition has historically led to both violent conflict (such as the Crusades or sectarian wars) and peaceful coexistence under frameworks of tolerance or pluralism [54, 55]. Notably, this competitive aspect mirrors ecological and epidemiological systems, where multiple strains or species vie for limited resources.

Religions also split and diversify, creating new sects, denominations, or entirely new movements [56, 57]. Schisms within Christianity, the formation of Sunni and Shia traditions in Islam, or the branching of Hindu and Buddhist schools illustrate how internal doctrinal disputes, leadership crises, or external pressures can fragment a religion into competing sub-groups. These splits often lead to rapid bursts of growth for the new branch, particularly when aligned with favorable social or political conditions. Such processes resemble mutation in biological systems, generating diversity within a lineage that can alter the competitive balance among strains.

Cycles of rise and decline are another recurrent pattern in religious history [58, 59]. New religious movements often begin as small, tightly bound communities, sometimes dismissed as cults or sects, but may grow rapidly when their message resonates with marginalized or disaffected groups [60]. Over time, some of these movements institutionalize and become dominant traditions, while others decline, fragment, or disappear altogether. The rise-and-fall cycles of millenarian cults, revivalist movements, and reformist sects highlight the temporal dynamics of religious spread and decline, often linked to broader socio-political turbulence.

Taken together, these insights point toward a few essential features of religion spread that are particularly relevant for formal modeling. First, religions diffuse through contact-like processes, influenced by networks of social interaction and mobility. Second, they compete as multiple strains within the same population, where outcomes can include coexistence, dominance, or extinction. Third, religions are subject to mutation-like splitting, producing new branches that alter the competitive landscape. Fourth, their dynamics exhibit cyclical rise-and-fall patterns, reflecting interactions between belief systems and broader socio-political forces. Finally, the rate and direction of spread are strongly modulated by external conditions—such as political stability, institutional regulation, and cultural diversity—which must therefore be incorporated into any realistic model of religious diffusion.

2.2 Epidemiological modeling

There are many types of modeling methods suggested in the literature to capture pandemic spread dynamics [61, 62, 63]. The simplest type of models are functional (phenomenological) models, which include logistic, Richards, Gompertz, and other growth curves fitting [64]. Other models focus on a bottom-to-top approach, simulating individual-level interactions to capture population-level spread dynamics with methods like the agent-based simulation [65, 66, 67]. Recently, data-driven models in general, and machine learning models such as ARIMA, tree ensembles, and deep recurrent/transformer models, in particular, gain more popularity due to the increased available computational power and better monitoring of modern pandemics [?]. Nevertheless, compartment models, such as the SIR model, are arguably still the most common type of epidemiological models due to their relatively high predictive power and explainable nature [68, 69]. In these models, one partitions the population into epidemiological states and describes flows between them via differential (or difference) equations [70].

The earliest example of a compartment model is the classical SIR model, which decomposes the population into three compartments: $S(t)$, $I(t)$, and $R(t)$ with dynamics described by the following system of ordinary differential equations (ODEs):

$$\frac{dS}{dt} = -\beta \frac{SI}{N}, \quad \frac{dI}{dt} = \beta \frac{SI}{N} - \gamma I, \quad \frac{dR}{dt} = \gamma I, \quad (1)$$

where $N = S + I + R$ is constant, $\beta > 0$ is the effective transmission rate, and $\gamma > 0$ is the recovery/removal rate [70]. This model, while appealing, more often than not, is unable to capture real-world epidemiological

dynamics. As such, many extensions have been proposed over the years that extend it to capture more realistic epidemiological dynamics. Most extensions are obtained by relaxing its simplifying assumptions, so it is useful to view them systematically. Common extensions: (i) add infection stages (e.g., exposed/latent, presymptomatic, asymptomatic) to represent progression and infection-to-infectiousness delays [71]; (ii) distinguish outcomes of infection (e.g., hospitalization, severe disease, death) as separate compartments rather than absorbing them into a single removed class [72]; (iii) introduce additional time scales via demographic turnover, waning immunity, or time-varying transmission such as seasonality [73]; and (iv) relax homogeneous mixing by incorporating population structure (age, risk, space), yielding coupled compartmental systems [74].

However, these extensions are still limiting the pandemic to a single pathogen. Real-world pandemics frequently involve multiple co-circulating strains (or variants) whose epidemiological parameters and immune-escape properties differ over time [75]. Extending single-strain compartmental models to multi-strain settings can be done at several levels of resolution, ranging from minimal “parallel-strain” models to history-based constructions that track immune states induced by prior infections.

A generic strategy is to represent strain identity explicitly (e.g., by duplicating infected compartments) and to encode immunological interactions using either (i) complete cross-immunity, (ii) partial cross-immunity through a susceptibility reduction matrix, or (iii) explicit immune-history compartments indexed by the set (or sequence) of previously experienced strains [76].

The most parsimonious multi-strain extension assumes that infection by any strain removes an individual from future susceptibility (i.e., no reinfection by any strain). Let $I_i(t)$ denote the number infectious with strain $i \in \{1, \dots, m\}$, with strain-specific transmission and recovery rates (β_i, γ_i) . A natural model is

$$\begin{aligned} \frac{dS}{dt} &= -\frac{S}{N} \sum_{i=1}^m \beta_i I_i, \\ \frac{dI_i}{dt} &= \beta_i \frac{SI_i}{N} - \gamma_i I_i, \quad i = 1, \dots, m, \\ \frac{dR}{dt} &= \sum_{i=1}^m \gamma_i I_i, \end{aligned} \tag{2}$$

where $N = S + \sum_i I_i + R$ is constant. This formulation captures competition for a shared susceptible pool and can generate strain replacement dynamics even without explicit reinfection. More realistic “no-reinfection” models often incorporate partial cross-immunity between strains at the transmission stage (while still preventing reinfection outcomes) [77, 78, 79].

Allowing reinfection requires relaxing the assumption that recovery permanently removes individuals from the susceptible class. Two common mechanisms are waning immunity and incomplete cross-immunity. In the first, individuals who recovered return to susceptibility over time while in the latter, prior infection reduces but does not eliminate susceptibility to the same or other strains. A convenient reduced description introduces strain-specific recovered classes R_i and permits infection of previously recovered individuals at a reduced rate. For example, letting $\sigma_{ij} \in [0, 1]$ denote the relative susceptibility to strain j after recovery from strain i , a schematic reinfection term takes the form $\beta_j \sigma_{ij} R_i I_j / N$. In its most general form, reinfection leads to immune-history indexing (e.g., R_J for individuals recovered from the set of strains J), which scales combinatorially with the number of strains and naturally encodes infection order [76]. Such models are useful when repeated infections materially affect population-level dynamics, including thresholds in which reinfection becomes dominant [80], strain invasion and

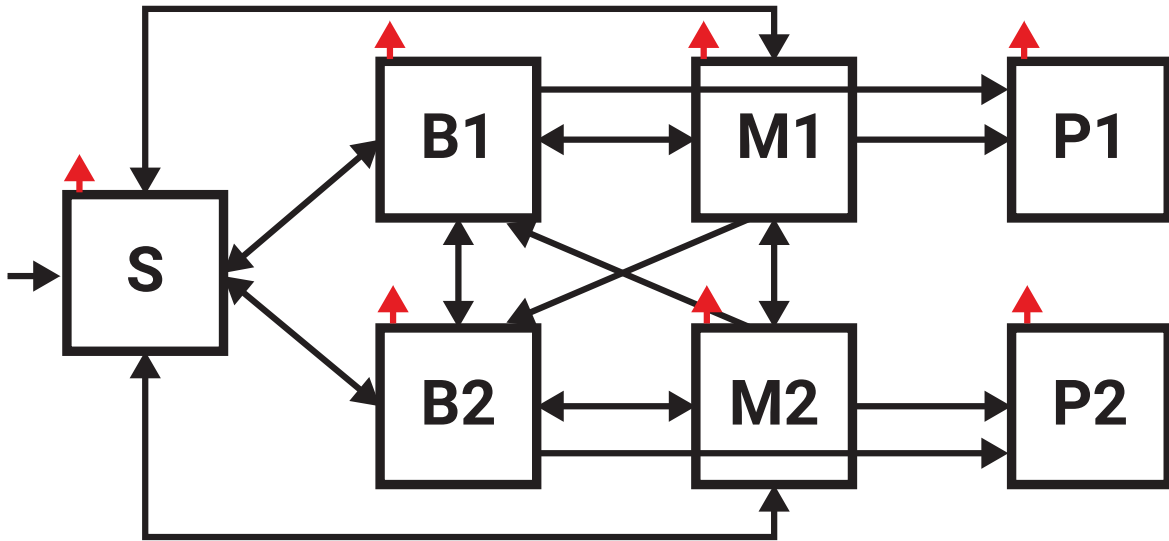


Figure 1: A schematic view of the model's structure for the case of two religions ($|\mathcal{R}| = 2$). Red (small, top-facing) arrows indicate death.

coexistence regimes [81], and settings where a newly emerging strain can effectively infect individuals with prior immunity [82].

Multi-strain models can treat strain appearance as exogenous where new strains are introduced at specified times or endogenous where new strains are generated by mutation from existing strains. A common endogenous representation is a mutation flow between infectious classes:

$$\frac{dI_i}{dt} = \dots - \sum_{j \neq i} \mu_{ij} I_i + \sum_{j \neq i} \mu_{ji} I_j, \quad (3)$$

where μ_{ij} is the rate at which infections of strain i generate infections of strain j (e.g., via within-host mutation and onward transmission). For many-strain settings, mutation is often coupled to antigenic distance so that both (a) mutation transitions and (b) cross-immunity depend on a strain-space metric. This yields a bridge between discrete multi-strain compartment models and evolutionary/antigenic-drift descriptions [83, 84, 85].

3 Model Definition

We model the spread of religions as a multi-strain epidemic process in which each religion plays the role of a distinct strain, and conversion is treated analogously to infection. The structure of the model combines (i) a multi-strain compartmental SIR framework, generalizing the approach of [76] and (ii) a time-varying, context-dependent transmission rate inspired by the EMIT social-epidemiological model [86]. In addition, we incorporate demographic turnover (birth and death) and “mutation” dynamics representing the emergence of new religions from existing ones [75]. Fig. 1 presents a schematic view of the model’s structure.

Formally, we consider a population with demographic turnover (birth and death) partitioned into a set of mutually exclusive compartments with pathogens that have a mutation mechanism. In this context, let $\mathcal{R} =$

$\{1, \dots, m\}$ denote a fixed set of modeled religions (some may have zero prevalence at a given time). At any time t , each individual is in exactly one of the following states: $S(t)$, $B_r(t)$, $M_r(t)$, and $P_r(t)$ such that $S(t)$ represents individuals without religion; $B_r(t)$ affiliated with religion $r \in \mathcal{R}$, but not actively trying to convert others (comparable to the exposed state in SEIS models); $M_r(t)$ affiliated with religion r and actively trying to convert others (comparable to the infectious state in SEIS models); $P_r(t)$ affiliated with religion r and serving as religious elite (unique to this model). The total population size is $N(t) = S(t) + \sum_{r \in \mathcal{R}} (B_r(t) + M_r(t) + P_r(t))$. By construction, each person can belong to at most one religion at a time; there are no co-infections by multiple religions.

To this end, we assume homogeneous mixing at the compartmental level [70]. The analogue of the “infectious” compartment in a standard SIR model is the set of missionaries $\{M_r\}_{r \in \mathcal{R}}$, who generate conversion attempts through social contact. Priests and non-proselytizing believers can indirectly affect conversion via the effective conversion rate, but do not directly act as “infectious” in the baseline model. Here, for each religion ($r \in \mathcal{R}$) we define a time-dependent “force of conversion” such that $\lambda_r(t) = \beta_r \frac{M_r(t)}{N(t)}$, where $\beta_r(t)$ is the effective per-contact conversion rate of religion r at time t . Note that $\lambda_r(t)$ depends only on missionaries in the numerator; priests P_r contribute only through $N(t)$ and do not directly generate conversion events.

Moreover, within each religion (r), individuals can move between behavioral roles - from passive believers to missionaries, and from either to priests. We use the following parameters: σ_r : rate at which passive believers become missionaries ($B_r \rightarrow M_r$); κ_r : rate at which missionaries cease active proselytizing and return to passive belief ($M_r \rightarrow B_r$); τ_r^B : rate at which passive believers become priests ($B_r \rightarrow P_r$); τ_r^M : rate at which missionaries become priests ($M_r \rightarrow P_r$). We also take into account a “disaffiliation” (apostasy) from each role at rates ρ_r^X moving from X to S for $X \in \{B, M, P\}$.

Missionaries of religion r may convert any individual who does not currently belong to r . The pool susceptible to r at time t is $X_r(t) = S(t) + \sum_{j \in \mathcal{R}, j \neq r} (B_j(t) + M_j(t))$, i.e. the non-affiliated and members of other religions who are not priests, which assumed not to switch religions.

We assume that newly converted individuals of religion r enter either the passive-believer or missionary compartment. Thus, let $q_r \in [0, 1]$ denote the probability that a new convert becomes a missionary; then $1 - q_r$ is the probability of entering as a passive believer. Using mass-action assumptions, the flow into religion r per unit of time is modeled as follows:

$$\lambda_r(t) X_r(t) = \beta_r(t) \frac{M_r(t)}{N(t)} \left[S(t) + \sum_{j \neq r} (B_j(t) + M_j(t)) \right].$$

This flow is split as

$$B_r : (1 - q_r) \lambda_r(t) X_r(t), \quad M_r : q_r \lambda_r(t) X_r(t). \quad (4)$$

Symmetrically, members of religion r can be converted away by missionaries of other religions. Each believer or missionary of r is exposed to conversion attempts from all other religions with total hazard $\sum_{\ell \neq r} \lambda_\ell(t)$, so the outflow from B_r and M_r due to cross-religious conversion is

$$B_r : B_r(t) \sum_{\ell \neq r} \lambda_\ell(t), \quad M_r : M_r(t) \sum_{\ell \neq r} \lambda_\ell(t), \quad (5)$$

with inflows into the corresponding B_ℓ and M_ℓ determined by the expressions above.

We include demographic turnover via per-capita birth and death rates b and μ . To reflect intergenerational transmission of religion, we assume that newborns inherit the religious identity and behavioral state of their parents in aggregate. Formally, we assume that births preserve the current composition of the population: at time t , the fraction of births entering compartment X equals $X(t)/N(t)$. Under this assumption, each compartment receives births at rate $b X(t)$ and loses individuals to natural death at rate $\mu X(t)$, so that

$$\frac{dN}{dt} = (b - \mu) N(t). \quad (6)$$

This is equivalent to assigning the same per-capita birth and death rates to all compartments while preserving the religious composition in expectation.

Religions may “mutate” by giving rise to new denominations and splinter groups. Thus, we introduce a mutation matrix $\nu_{r\ell} \geq 0$ ($r \neq \ell$), where $\nu_{r\ell}$ denotes the rate at which a missionary switches/relabels from religion r to ℓ (i.e., a transfer $M_r \rightarrow M_\ell$ within the modeled set \mathcal{R}). Notably, we assume that mutation acts only on missionaries, as they are the most active in redefining and propagating doctrine. Formally, the mutation term in the equation for M_r is

$$\left(\frac{dM_r}{dt} \right)_{\text{mut}} = \sum_{\ell \neq r} \nu_{\ell r} M_\ell(t) - \sum_{\ell \neq r} \nu_{r\ell} M_r(t). \quad (7)$$

Taken jointly, the system of ODEs (ODEs) is for each religion ($r \in \mathcal{R}$) takes the form:

$$\frac{dS}{dt} = b S - \mu S - S \sum_{k \in \mathcal{R}} \lambda_k(t) + \sum_{k \in \mathcal{R}} (\rho_k^B B_k + \rho_k^M M_k + \rho_k^P P_k), \quad (8)$$

$$\begin{aligned} \frac{dB_r}{dt} &= b B_r - \mu B_r + (1 - q_r) \lambda_r(t) \left[S + \sum_{j \neq r} (B_j + M_j) \right] - B_r \sum_{\ell \neq r} \lambda_\ell(t) \\ &\quad - \sigma_r B_r + \kappa_r M_r - \rho_r^B B_r - \tau_r^B B_r, \end{aligned} \quad (9)$$

$$\begin{aligned} \frac{dM_r}{dt} &= b M_r - \mu M_r + q_r \lambda_r(t) \left[S + \sum_{j \neq r} (B_j + M_j) \right] - M_r \sum_{\ell \neq r} \lambda_\ell(t) \\ &\quad + \sigma_r B_r - \kappa_r M_r - \rho_r^M M_r - \tau_r^M M_r \\ &\quad + \sum_{\ell \neq r} \nu_{\ell r} M_\ell - \sum_{\ell \neq r} \nu_{r\ell} M_r, \end{aligned} \quad (10)$$

$$\frac{dP_r}{dt} = b P_r - \mu P_r + \tau_r^B B_r + \tau_r^M M_r - \rho_r^P P_r. \quad (11)$$

4 Model Analysis

In this section, we analyze the proposed model through a sequence of experiments designed to evaluate both its descriptive realism and its explanatory and predictive utility. We first outline the experimental design, including the simulation protocol, parameterization strategy, and the summary statistics used to compare model outputs to empirical patterns. We then present results from three complementary experiment types: (i) stylized forward simulations demonstrating that the model reproduces qualitative religion dynamics commonly observed in real

populations (e.g., emergence, rapid expansion, coexistence, replacement, and persistence under competition); (ii) historical case studies showing that the model can be calibrated to match documented shifts in religious composition and that the inferred mechanisms provide interpretable explanations for the observed transitions; and (iii) a sensitivity analysis mapping how key parameters govern regime changes, enabling controlled movement between distinct dynamical outcomes.

4.1 Experimental design

We evaluate the model using a common set of mechanisms across all experiments; Scenarios A–C differ only in parameter values and initial conditions, with no scenario-specific rules. The experiments pursue three objectives: (i) illustrate how the same dynamical structure can generate qualitatively distinct diffusion trajectories under different parameter regimes (Scenarios A–C); (ii) assess empirical plausibility by calibrating simplified variants to historical affiliation records, using three real-world cases: Sweden (Church of Sweden, Svenska kyrkan), a high-demand movement with annual diffusion statistics (Jehovah’s Witnesses), and a country-level replacement setting based on census tabulations (New Zealand religious affiliation). In these settings, we compared time-invariant baselines to piecewise-constant rate specifications; and (iii) characterized regime boundaries by mapping qualitative outcomes for an emergent religion across a two-parameter grid, providing phase intuition via a heatmap. Technically, we use a common simulation and reporting protocol across all experiments in which, for any fixed parameterization, we run the ABS with time step $\Delta t = 0.1$ and population size $N(0) = 10000$. The ABS is repeated for $R = 100$ independent replicates, and we report replicate-mean trajectories unless stated otherwise. The solver is implemented in the Python programming language (v3.11.5) [87].

4.1.1 Reproducing religion spread dynamics

We define three representative parameterizations that generate qualitatively distinct religion dynamics within the same model. In all scenarios, the initial condition is specified by integer counts for susceptibles $S(0)$ and, for each religion r , the compartment sizes $B_r(0)$, $M_r(0)$, and $P_r(0)$. Scenarios differ only through parameter values and initial seeding; no additional rules are introduced. Exact settings are provided in the Appendix (Table 1).

Scenario A (emergence and takeover). We consider the endogenous emergence of a new major religion. Religion $r = 1$ is initially dominant (high $y_1(0)$), while religion $r = 2$ is absent at $t = 0$, i.e., $B_2(0) = M_2(0) = P_2(0) = 0$. Religion 2 appears through mutation-mediated schism, modeled as relabeling of religion-1 missionaries to religion 2 at rate $\nu^{(1 \rightarrow 2)} = 0.002 \text{ yr}^{-1}$. Parameters are then chosen so that the new religion has a net advantage in growth and persistence—for instance, higher baseline conversion strength ($\beta_{2,0} = 0.45$ vs. $\beta_{1,0} = 0.30$) together with lower attrition—so that it can expand from rarity and ultimately replace (or strongly compete with) the incumbent.

Scenario B (transient cults). We study the repeated appearance and disappearance of small, short-lived groups. Religion $r = 1$ is initialized as the dominant tradition, while a set of potential “cult” strains $r \in \{2, \dots, 6\}$ start at zero prevalence: $B_r(0) = M_r(0) = P_r(0) = 0$. These strains are introduced endogenously via schism from religion 1, with missionaries relabeling to each $r \geq 2$ at rate $\nu^{(1 \rightarrow r)} = 0.005 \text{ yr}^{-1}$. Their parameters are selected to make sustained growth unlikely: weaker conversion ($\beta_{r,0} = 0.18 < \beta_{1,0} = 0.30$), higher disaffiliation ($\rho_B^{(r)} = \rho_M^{(r)} = 0.02$ vs. 0.006 for religion 1), limited institutional progression ($\tau_B^{(r)} = \tau_M^{(r)} = 0.0005$ vs. $\tau_B^{(1)} = 0.002$ and $\tau_M^{(1)} = 0.003$), and faster reversion from missionary to believer ($\kappa_r = 0.04 > \kappa_1 = 0.02$).

Under this regime, secondary strains tend to exhibit low-prevalence, short-duration bursts, while the dominant religion remains comparatively stable over the simulated horizon.

Scenario C (long-run coexistence). We probe sustained coexistence under a near-symmetric specification in which neither religion has a systematic advantage. Both religions are present at $t = 0$: religion 1 starts with $(B_1(0), M_1(0), P_1(0)) = (2000, 120, 180)$ and religion 2 with $(B_2(0), M_2(0), P_2(0)) = (1200, 80, 120)$, with $S(0) = 6500$ (so $N_0 = 10200$). Baseline conversion strengths are close ($\beta_{1,0} = 0.28$, $\beta_{2,0} = 0.26$), and all remaining behavioral and attrition parameters are matched across religions: $q_1 = q_2 = 0.05$, $\sigma_1 = \sigma_2 = 0.018$, $\kappa_1 = \kappa_2 = 0.018$, $\tau_B^{(1)} = \tau_B^{(2)} = 0.0015$, $\tau_M^{(1)} = \tau_M^{(2)} = 0.0020$, $\rho_B^{(1)} = \rho_B^{(2)} = 0.006$, $\rho_M^{(1)} = \rho_M^{(2)} = 0.006$, and $\rho_P^{(1)} = \rho_P^{(2)} = 0.001$. We include small symmetric schism rates $\nu^{(1 \rightarrow 2)} = \nu^{(2 \rightarrow 1)} = 0.0002$ and fix demographic turnover at $b = \mu = 0.01$. To assess asymptotic behavior, we simulate this balanced regime over a long horizon ($T = 216$ weeks) with step size $\Delta t = 1$ day.

4.1.2 Historical-record fitting

We use three historically grounded datasets that support later calibration at different temporal resolutions: **Sweden (state-church decline).** We fit to the annual membership share of the Church of Sweden (Svenska kyrkan), using the official series “Medlemmar % av folkmängden” reported for 1972–2024 [88]. The source notes that 1981 is missing (no population register was produced), and we therefore omit that year rather than interpolate [88]. In the proof-of-concept, we fix a single breakpoint at $t^* = 2000$ and assess whether a post-2000 change in effective rates improves fit relative to the time-invariant baseline.

High-demand movement / “cult”-like diffusion As a candidate setting with systematically reported annual diffusion metrics, we use the *Service Year Report* of Jehovah’s Witnesses, which provides yearly global totals and detailed country/territory tables [89]. The country/territory tables include population alongside annual and peak counts of active publishers, enabling direct construction of time series of shares (publisher-to-population ratios) for multiple regions [90]. This setting supports calibration of rapid-growth, saturation, and stagnation/decline regimes within a consistent reporting framework.

Religion replacement at the country level (secularization and switching). To study replacement dynamics (e.g., Christianity declining while the share reporting “no religion” rises), we use New Zealand census tabulations of religious affiliation across the 2001, 2006, 2013, 2018, and 2023 censuses, distributed by Stats NZ and made available as a downloadable table [91]. We work with national totals and compute shares relative to the “total people stated” denominator for each census year. This yields a low-frequency but nationally representative time series suitable for fitting two-strain or “religion vs. none” variants, and for benchmarking replacement-like transitions.

The fitting procedure used to fit the proposed model’s parameters to the historical records is provided in the Appendix.

4.1.3 Phase transition

To develop intuition for the three qualitative regimes studied above, we perform a sensitivity analysis that varies two influential parameters of the focal (new) religion in the Scenario A configuration: its baseline conversion strength $\beta_{0,2}$ and its missionary disaffiliation rate ρ_2^M . All remaining parameters and initial conditions are fixed at their Scenario A values. Consequently, we sweep a 10×10 grid of parameter pairs $(\beta_{0,2}, \rho_2^M)$ over predefined bounded ranges. For each grid cell, we run $R = 100$ independent ABS replicates with step size $\Delta t = 0.1$ over a horizon of $T = 216$ weeks, and compute the replicate-mean share trajectory of the total population share of

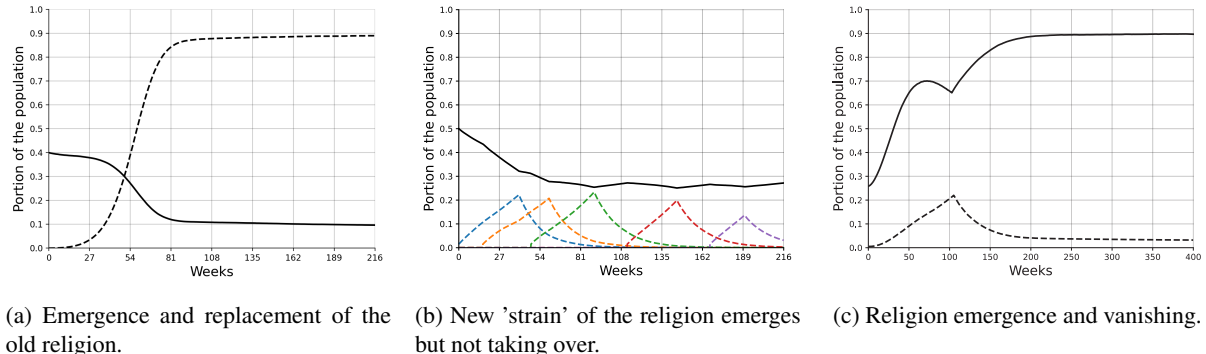
the second religion. Regime labels are determined from the terminal portion of the trajectory - the final 20% of simulated time points. Formally, let y_{final} be the mean of $y_2(t)$ over this window, and let stab be the corresponding standard deviation. We classify outcomes as: (A) *takeover/large* if $y_{\text{final}} \geq 0.30$; (C) *stable coexistence* if $0.02 \leq y_{\text{final}} < 0.30$ and $\text{stab} \leq 0.005$; and (B) *small/transient* otherwise.

4.2 Results

This section reports the experiments' obtained results. We first show that the model reproduces canonical qualitative regimes observed in real religious dynamics, then demonstrate that reduced-form calibrations match historical affiliation records, and finally map regime transitions in parameter space to identify the conditions under which emergence leads to persistence, coexistence, or takeover.

4.2.1 Stylized simulations reproduce canonical religion dynamics

Fig. 2 presents replicate-mean time-series of population shares under three stylized parameterizations (Scenarios A–C), illustrating how the same mechanistic model yields distinct macrodynamics under changes in parameters and initial conditions. Panel (a) shows the emergence of a new religion (strain) that starts at (near) zero prevalence and grows to dominate the population; panel (b) shows repeated transient waves of multiple minor strains that peak and then fade; and panel (c) shows a boom–bust episode in which a challenger briefly expands but then effectively goes extinct, leaving a near-stationary dominant composition. In Fig. 2a, we observe a characteristic “establishment-from-rarity” trajectory: religion 2 remains near zero initially (mutation-mediated seeding), then passes a takeoff point where growth accelerates, followed by saturation as competition intensifies. Quantitatively, religion 2 crosses the 1% threshold at $t = 17.6$ weeks, reaches parity with religion 1 at $t = 49.9$ weeks, and ends at $y_1 = 0.096$ and $y_2 = 0.890$ at $T = 216$ weeks. In Fig. 2b, the dominant religion remains bounded while five minor strains generate transient “cult-like” waves; the simulation produces five distinct bursts, with the largest minor strain peaking at about 0.23–0.25, and the combined final share of all minor strains at $T = 216$ weeks remaining small (around 0.03). In Fig. 2c, the challenger rises from its initial seed to a transient peak (around $t = 100$ weeks) but then steadily collapses toward 0.04 of the population and stabilizes at this rate. In contrast, religion 1 approaches a dominant plateau around 0.90 and remains effectively stationary thereafter.



(a) Emergence and replacement of the old religion. (b) New ‘strain’ of the religion emerges but not taking over. (c) Religion emergence and vanishing.

Figure 2: Replicate-mean population-share trajectories for three stylized parameterizations.

4.2.2 Historical-record fitting

Fig. 3 presents three historical-record fitting case studies, each comparing the observed affiliation share (points) to fitted trajectories from the reduced calibration model introduced in the experimental design (Eq. (13)). Specifically, in Fig. 3a, we observe a long-run decline whose slope changes over time: the stationary baseline captures the overall direction but systematically underfits the post-break segment, whereas the piecewise model aligns closely with both the pre-break and post-break phases. The Sweden church membership series spans 1972–2024 (52 observation points, excluding 1981) with a fixed breakpoint at $t^* = 2000$; the stationary baseline attains $R^2 = 0.818$ (MAE = 0.052), while the piecewise model improves to $R^2 = 0.978$ (MAE = 0.016). In Fig. 3b, we see a growth process that slows and stabilizes: the fitted trajectory reproduces the early increase and the later saturation/plateau by shifting the balance between effective recruitment and attrition at the breakpoint, yielding the desired agreement with the observed inflection. The Turkey Jehovah’s Witnesses series covers 2014–2024 (11 observation points) and is fit with a logistic-capacity variant (fitted $K = 1.2 \times 10^{-4}$) and a breakpoint at $t^* = 2021$; the baseline yields $R^2 = 0.912$ (MAE = 2.90×10^{-6}) and the piecewise fit yields $R^2 = 0.924$ (MAE = 2.87×10^{-6}). In Fig. 3c, we observe a rise-and-fall pattern consistent with short-lived expansion followed by decline; the fitted model tracks both the upswing and the subsequent downturn by allowing the post-break regime to invert the net growth (e.g., by increasing ρ and/or decreasing β). The New Zealand “no religion” share is defined as none_count/total_stated over five census years (2001, 2006, 2013, 2018, 2023); selecting $t^* = 2013$ via grid search over {2006, 2013, 2018} improves the fit from $R^2 = 0.997$ (MAE = 0.0037) to $R^2 = 1.000$ (MAE = 2.99×10^{-6}). Given the small number of census points, we interpret this as a descriptive goodness-of-fit check rather than a high-resolution calibration. The obtained model’s parameters’ values for all three cases are provided in the Appendix.

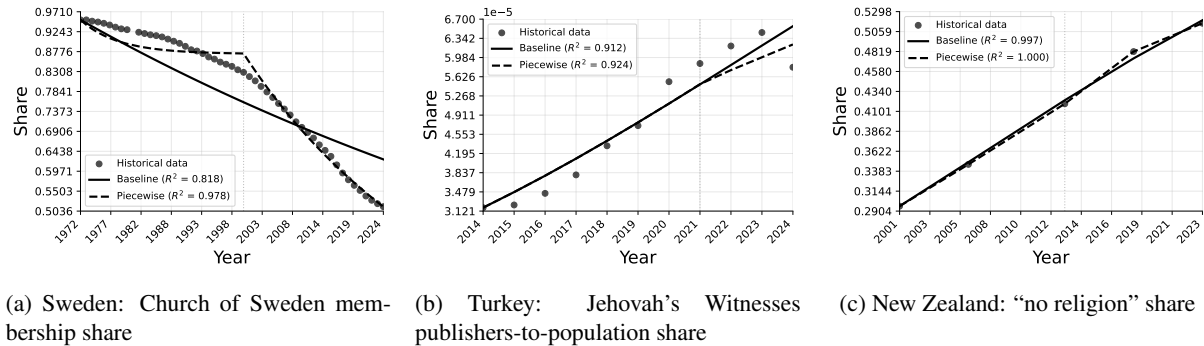


Figure 3: Historical-record fitting case studies.

4.2.3 Phase transition

Fig. 4 shows a well-structured phase diagram with three clearly separated regimes. A sufficiently high baseline conversion rate of the new religion ($\beta_{0,2}$) produces near-certain takeover, largely independent of the missionary disaffiliation rate ρ_2^M . In contrast, low conversion strength leads to a small or transient (“cult”) outcome, particularly when ρ_2^M is non-negligible. Stable coexistence occupies an intermediate band of parameter space, spanning a wide range of ρ_2^M values but only moderate $\beta_{0,2}$. In the current run, takeover outcomes occupy roughly a third of the grid, stable coexistence about half, and small/transient outcomes the remaining sixth. The transition between

coexistence and takeover is sharp and nearly vertical: around $\beta_{0,2} = 0.40-0.43$, an increase in conversion strength of only 0.02-0.03 (holding ρ_2^M fixed) is sufficient to move the system from long-run coexistence to near-total dominance of the new religion, corresponding to changes in terminal mean share on the order of 10 to 20 percentage points. This sharp boundary supports the interpretation of a genuine phase transition, where modest socio-political shifts affecting recruitment efficacy can qualitatively reshape the long-run religious landscape.

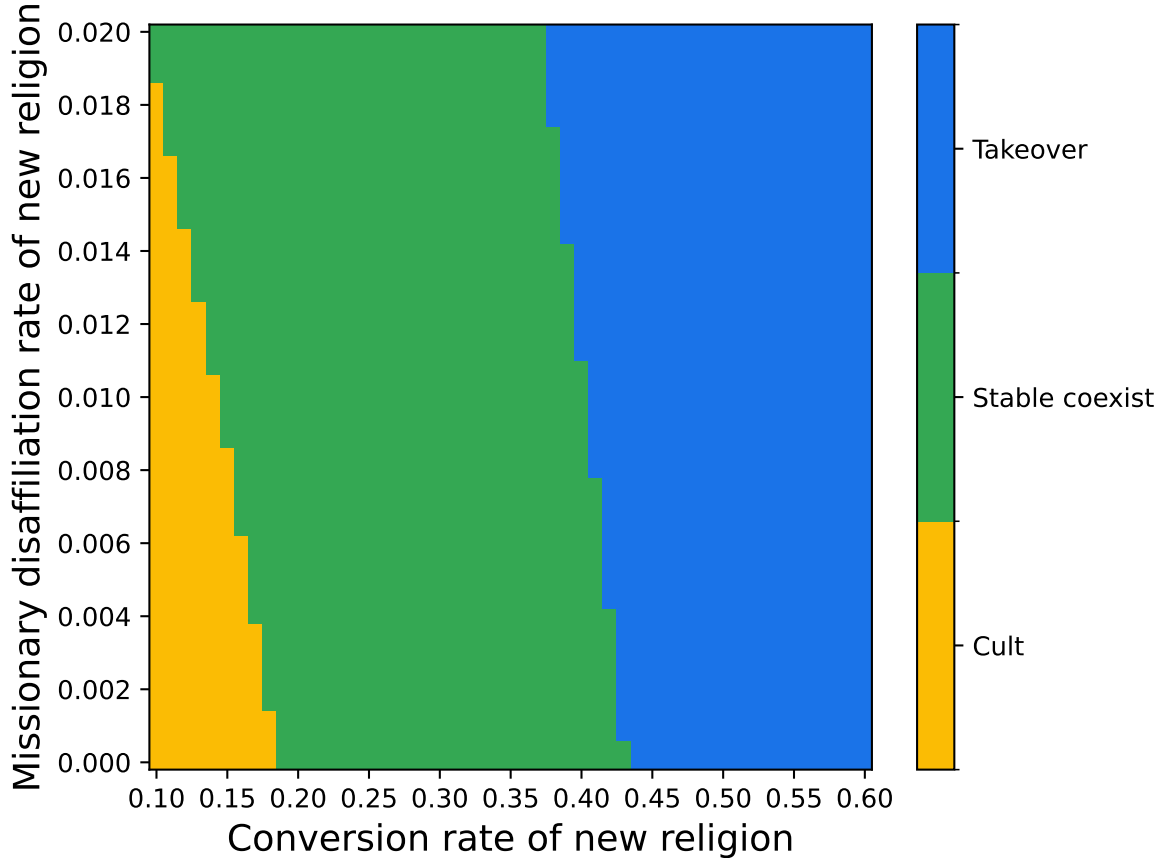


Figure 4: Religion spread dynamics phase transition based on baseline conversion strength and missionary disaffiliation.

5 Discussion

In this study, we introduce an epidemiologically inspired framework for modeling religious dynamics as a multi-strain contagion process with role heterogeneity and endogenous emergence through mutation-like splitting. Building on classical compartment modeling and cultural-diffusion perspectives, the model formalizes conversion as a contact-driven process while allowing social context to modulate effective transmission over time.

Our results provide evidence that the proposed mechanism can generate the key qualitative patterns that motivate epidemiological analogies in the first place: emergence and replacement, transient rise-and-fall waves, and stable coexistence. These regimes mirror well-established findings from diffusion and cultural transmission re-

search, where adoption trajectories can range from rapid takeoff to plateauing and decline depending on social reinforcement and retention pressures [92, 93, 94]. In particular, the threshold-like boundaries observed in the phase map align with the view that many social behaviors behave as “complex contagions” requiring reinforcement and exhibiting strong sensitivity to local conditions [95]. Interpreted sociologically, the model’s parameters provide a compact language for expressing mechanisms discussed in the religion literature, including competition in a shared adherent pool and the role of organizational strength and retention [96]. The historical-record fits further support the central claim that secularization-like trajectories can often be summarized as regime shifts in effective rates: a minimal piecewise specification captures accelerated decline without requiring additional ad hoc structure, which is consistent with long-running accounts of modernity-driven institutional weakening and changing existential security [97, 98].

Beyond predictive accuracy, the model can serve as a practical tool for sociological inquiry in at least three ways. First, it can be used for mechanism testing where competing hypotheses about why a religion grows or declines, can be mapped onto distinct parameter changes and then evaluated by comparing the resulting trajectories to empirical time series. Second, it supports comparative analysis. Namely, by fitting the same formal structure across countries or periods, researchers and practitioners can compare inferred rate profiles and relate them to macro covariates such as education, state policy, media ecosystems, or social heterogeneity, thereby linking descriptive trends to interpretable mechanisms in a principled way [92, 98]. Third, it provides a counterfactual simulator. Once calibrated, the model can be used to explore “what-if” scenarios such as changes in conversion opportunities, regulation, or schism propensity and examine how close a given setting may be to a qualitative regime boundary, in the same spirit that epidemiological models support policy reasoning. Methodologically, this agenda fits naturally into broader work that treats the spread of socially transmitted states (ideas, behaviors, rumors) with epidemic-style formalisms [99, 100, 101, 102].

This study is not without limitations. First, the baseline model assumes homogeneous mixing, while real conversion processes occur on structured social networks; incorporating explicit network or spatial structure would allow the model to represent clustered reinforcement and long-tie effects more directly [95]. Moreover, the introduction of a spatial component to the model [103, 104] can allow the exploration of population migrations, such as historical armies like the Christian crusades [105] or recent Muslim migration into Europe [106]. Second, individuals are restricted to a single affiliation at a time, excluding syncretism, dual practice, and layered identity; extending the state space to allow partial or multi-affiliation can capture more complex social identity in individuals. Third, parameter identifiability is a practical challenge: multiple mechanisms can produce similar aggregate curves, especially when only low-frequency data are available. Future work should incorporate richer observables and adopt Bayesian or hierarchical calibration to better quantify uncertainty and enable cross-context pooling [93]. Finally, demography is simplified by composition-preserving births and uniform death rates; adding age structure, migration, and cohort effects could help explain long-run secularization patterns that are known to vary by generation [98].

Taken jointly, the proposed model offers a flexible and interpretable bridge between qualitative theories of religious change and quantitative dynamical modeling. By showing that a single mechanistic framework can reproduce the regimes we care about, fit historically grounded trajectories under parsimonious nonstationarity, and expose meaningful regime boundaries in parameter space, this study provides a foundation for treating religious dynamics as a measurable, comparable, and hypothesis-generating diffusion process. This opens a path toward a cumulative research program in which sociological theories of conversion, competition, and institutionalization

can be expressed as model mechanisms, tested against data, and compared across settings in a transparent way.

Declarations

Funding

This study received no funding.

Code availability

The code used for this study is freely available at: <https://github.com/bilgesi/religion-dynamics-ode-abs>.

Conflicts of Interest/Competing Interests

The author declares no conflict of interest.

Author contribution

Bilge Taskin: Software, Formal analysis, Investigation, Data Curation, Writing - Review & Editing, Visualization.
 Teddy Lazebnik: Conceptualization, Methodology, Validation, Writing - Original Draft, Writing - Review & Editing, Visualization, Supervision.

References

- [1] Mark Juergensmeyer. *Religion in global civil society*. Oxford University Press, 2005.
- [2] Meredith B McGuire. *Religion: The social context*. Waveland Press, 2008.
- [3] Robert N Bellah. *Beyond belief: Essays on religion in a post-traditionalist world*. Univ of California Press, 1991.
- [4] Martin Lang. The evolutionary paths to collective rituals: An interdisciplinary perspective on the origins and functions of the basic social act. *Archive for the Psychology of Religion*, 41(3):224–252, 2019.
- [5] Martin D Stringer. Building on belief: Defining animism in tylor and contemporary society. In *The handbook of contemporary animism*, pages 63–72. Routledge, 2014.
- [6] Lance Grande. *The evolution of religions: A history of related traditions*. Columbia University Press, 2024.
- [7] Tammi J Schneider. *An introduction to ancient Mesopotamian religion*. Wm. B. Eerdmans Publishing, 2011.
- [8] Emily Teeter. *Religion and ritual in ancient Egypt*. Cambridge University Press, 2011.
- [9] Upinder Singh. *The Idea of Ancient India: Essays on Religion, Politics and Archaeology*. Penguin Random House India Private Limited, 2023.

- [10] Carlton H Tucker. From the axial age to the new age: Religion as a dynamic of world history. *The History Teacher*, 27(4):449–464, 1994.
- [11] Jan Assmann. World religions and the theory of the axial age. *Dynamics in the History of Religions*, 1, 2012.
- [12] Abbas Mirakhor and Hossein Askari. Conception of justice: Axial age—india, china and greece. In *Conceptions of Justice from Earliest History to Islam*, pages 115–164. Springer, 2019.
- [13] Dorothea Weltecke. The medieval period. *The Oxford Handbook of Atheism*, pages 164–178, 2013.
- [14] Clifford Hugh Lawrence and Janet Burton. *Medieval monasticism: forms of religious life in Western Europe in the Middle Ages*. Routledge, 2023.
- [15] Edward Grant. Science and religion, 400 bc to ad 1550: from aristotle to copernicus. 2006.
- [16] Tuomas Martikainen. The global political economy, welfare state reforms, and the governance of religion. In *Post-Secular Society*, pages 71–93. Routledge, 2017.
- [17] François Gauthier. *Religion in the neoliberal age: Political economy and modes of governance*. Routledge, 2016.
- [18] Peter L Berger. The desecularization of the world: A global overview. *The new sociology of knowledge*, pages 61–76, 2017.
- [19] Gabriel A Almond, R Scott Appleby, and Emmanuel Sivan. *Strong religion: The rise of fundamentalisms around the world*. University of Chicago Press, 2011.
- [20] Nikki R Keddie. The new religious politics: where, when, and why do “fundamentalisms” appear? *Comparative studies in society and history*, 40(4):696–723, 1998.
- [21] Manuel A Vásquez. Religion, globalization, and migration. In *Religions in the Modern World*, pages 431–452. Routledge, 2016.
- [22] Ruth Tsuria and Aya Yadlin-Segal. Digital religion and global media: Flows, communities, and radicalizations. *Handbook of global media ethics*, pages 157–175, 2021.
- [23] Michael Wilkinson. The emergence, development, and pluralisation of global pentecostalism. In *Handbook of Global Contemporary Christianity*, pages 93–112. Brill, 2015.
- [24] Enzo Pace. The catholic charismatic movement in global pentecostalism. *Religions*, 11(7):351, 2020.
- [25] Allan Anderson, Michael Bergunder, Andre F Droogers, and Cornelis Van der Laan. *Studying global Pentecostalism: Theories and methods*, volume 10. Univ of California Press, 2010.
- [26] Clive D Field. *Counting religion in Britain, 1970-2020: secularization in statistical context*. Oxford University Press, 2021.
- [27] Amr Sabet. Religion, politics and social change: A theoretical framework. *Religion, State and Society: The Keston Journal*, 24(2-3):241–268, 1996.

- [28] Mehmet Karaçuka. Religion and economic development in history: Institutions and the role of religious networks. *Journal of Economic Issues*, 52(1):57–79, 2018.
- [29] Robert L Montgomery. The spread of religions and macrosocial relations. *Sociological Analysis*, 52(1):37–53, 1991.
- [30] Robert L Montgomery. Special persons and the spread of religions. *Pastoral psychology*, 65(3):369–393, 2016.
- [31] Safina Safitri. The role of social media in spreading religious moderation values. *Young Journal of Social Sciences and Humanities*, 1(1):99–107, 2025.
- [32] Augustine WC Msiska. The spread of islam in malawi and its impact on yao rites of passage, 1870-1960. *The Society of Malawi Journal*, 48(1):49–86, 1995.
- [33] John Hayward. Mathematical modeling of church growth. *The Journal of mathematical sociology*, 23(4):255–292, 1999.
- [34] Alaa Mujallad and Haitham Khoj. Is there hope for the hajj? using the sir model to forecast covid-19 progression in the city of makkah. *medRxiv*, 2020.
- [35] Matteo Castiello, Dajana Conte, and Samira Iscaro. Using epidemiological models to predict the spread of information on twitter. *Algorithms*, 16(8), 2023.
- [36] Michael Doebeli and Iaroslav Ispolatov. A model for the evolutionary diversification of religions. *arxiv*, 2008.
- [37] Michael A Cretacci. Religion and social control: An application of a modified social bond on violence. *Criminal Justice Review*, 28(2):254–277, 2003.
- [38] Edward Alsworth Ross. Social control. v. religion. *American journal of sociology*, 2(3):433–445, 1896.
- [39] Anneli Kaasa. Religion and social capital: Evidence from european countries. *International Review of Sociology*, 23(3):578–596, 2013.
- [40] Mircea Eliade. *A history of religious ideas volume 1: From the Stone age to the Eleusinian mysteries*, volume 1. University of Chicago Press, 2020.
- [41] Richard Sosis and Bradley J Ruffle. Ideology, religion, and the evolution of cooperation: Field experiments on israeli kibbutzim. In *Socioeconomic aspects of human behavioral ecology*, pages 89–117. Emerald Group Publishing Limited, 2004.
- [42] Joseph Bulbulia. Spreading order: religion, cooperative niche construction, and risky coordination problems. *Biology & Philosophy*, 27(1):1–27, 2012.
- [43] Andrew Phillips. *War, religion and empire: The transformation of international orders*, volume 117. Cambridge University Press, 2010.
- [44] Richard Sosis. Does religion promote trust?: The role of signaling, reputation, and punishment. *Interdisciplinary journal of research on religion*, 1, 2005.

- [45] Gary D Bouma. Religious resurgence, conflict and the transformation of boundaries. *P. Beyer & L. Beaman, Religion, Globalization, and Culture. Leiden and Boston: Brill*, pages 187–202, 2007.
- [46] Andreas Hasenclever and Volker Rittberger. Does religion make a difference? theoretical approaches to the impact of faith on political conflict. *Millennium*, 29(3):641–674, 2000.
- [47] Wade Clark Roof. Religion and narrative. *Review of religious research*, 34(4):297–310, 1993.
- [48] Yosef Garfinkel. *Dancing at the Dawn of Agriculture*. University of Texas Press, 2010.
- [49] Dana L Haggard and Stephen Haggard. Governance, law, religion and culture. *International Journal of Organization Theory & Behavior*, 13(4):569–596, 2010.
- [50] Teddy Lazebnik, Labib Shami, and Svetlana Bunimovich-Mendrazitsky. A hybrid mathematical model for an optimal border closure policy during a pandemic. *International Journal of Applied Mathematics and Computer Science*, 33(4), 2023.
- [51] Richard Foltz. Religions of the silk road. *New York: St. Martin's Griffin*, 1999.
- [52] Johan Elverskog. *Buddhism and Islam on the silk road*. University of Pennsylvania press, 2011.
- [53] Robert L Montgomery. The spread of religions and macrosocial relations. *Sociological Analysis*, 52(1):37–53, 1991.
- [54] Roger Finke. The consequences of religious competition: Supply-side explanations for religious change. In *Rational choice theory and religion*, pages 46–65. Routledge, 2016.
- [55] Jonathan Fox. A world survey of secular-religious competition: state religious policy from 1990 to 2014. In *The Correlates of Religion and State*, pages 9–28. Routledge, 2020.
- [56] Eileen Barker. Revision and diversification in new religious movements: an introduction. In *Revisionism and diversification in new religious movements*, pages 1–14. Routledge, 2016.
- [57] James R Lewis and Sarah M Lewis. *Sacred schisms: how religions divide*. Cambridge University Press, 2009.
- [58] Barbara Diefendorf. Were the wars of religion about religion? *political theology*, 15(6):552–563, 2014.
- [59] Norman Housley. *Religious warfare in Europe 1400-1536*. OUP Oxford, 2008.
- [60] J Gordon Melton and James R Lewis. Birth of a religion. *Scientology*, pages 17–33, 2009.
- [61] Lu Tang, Yiwang Zhou, Lili Wang, Soumik Purkayastha, Leyao Zhang, Jie He, Fei Wang, and Peter X-K Song. A review of multi-compartment infectious disease models. *International Statistical Review*, 88(2):462–513, 2020.
- [62] Sheryl L Chang, Mahendra Piraveenan, Philippa Pattison, and Mikhail Prokopenko. Game theoretic modelling of infectious disease dynamics and intervention methods: a review. *Journal of biological dynamics*, 14(1):57–89, 2020.

- [63] Philip E Paré, Carolyn L Beck, and Tamer Başar. Modeling, estimation, and analysis of epidemics over networks: An overview. *Annual Reviews in Control*, 50:345–360, 2020.
- [64] Teddy Lazebnik. Computational applications of extended SIR models: A review focused on airborne pandemics. *Ecological Modelling*, 483:110422, 2023.
- [65] Teddy Lazebnik. Evaluating supply chain resilience during pandemic using agent-based simulation. *Physica A: Statistical Mechanics and its Applications*, page 130780, 2025.
- [66] Cliff C Kerr, Robyn M Stuart, Dina Mistry, Romesh G Abeysuriya, Katherine Rosenfeld, Gregory R Hart, Rafael C Núñez, Jamie A Cohen, Prashanth Selvaraj, Brittany Hagedorn, et al. Covasim: an agent-based model of covid-19 dynamics and interventions. *PLOS Computational Biology*, 17(7):e1009149, 2021.
- [67] Petrônio CL Silva, Paulo VC Batista, Hélder S Lima, Marcos A Alves, Frederico G Guimarães, and Rodrigo CP Silva. Covid-abs: An agent-based model of covid-19 epidemic to simulate health and economic effects of social distancing interventions. *Chaos, Solitons & Fractals*, 139:110088, 2020.
- [68] Peijue Zhang, Kairui Feng, Yuqing Gong, Jieon Lee, Sara Lomonaco, and Liang Zhao. Usage of compartmental models in predicting covid-19 outbreaks. *The AAPS Journal*, 24(5):98, 2022.
- [69] Fatemeh Mirsaedi, Mohammad Sheikhalishahi, Mehrdad Mohammadi, Amir Pirayesh, and Dmitry Ivanov. Compartmental models in epidemiology: bridging the gap with operations research for enhanced epidemic control. *Annals of Operations Research*, pages 1–58, 2025.
- [70] W. O. Kermack and A. G. McKendrick. A contribution to the mathematical theory of epidemics. *Proceedings of the Royal Society*, 115:700–721, 1927.
- [71] Teddy Lazebnik, Labib Shami, and Svetlana Bunimovich-Mendrazitsky. Intervention policy influence on the effect of epidemiological crisis on industry-level production through input–output networks. *Socio-Economic Planning Sciences*, page 101553, 2023.
- [72] Teddy Lazebnik, Labib Shami, and Svetlana Bunimovich-Mendrazitsky. Spatio-temporal influence of non-pharmaceutical interventions policies on pandemic dynamics and the economy: the case of COVID-19. *Economic Research-Ekonomska Istraživanja*, 35(1):1833–1861, 2022.
- [73] Herbert W. Hethcote. The mathematics of infectious diseases. *SIAM Review*, 42(4):599–653, 2000.
- [74] Adi Shuchami and Teddy Lazebnik. Spatio-temporal sir model of pandemic spread during warfare with optimal dual-use health care system administration using deep reinforcement learning. *Disaster Medicine and Public Health Preparedness*, 19:e197, 2025.
- [75] Labib Shami and Teddy Lazebnik. Economic aspects of the detection of new strains in a multi-strain epidemiological–mathematical model. *Chaos, Solitons & Fractals*, 165:112823, 2022.
- [76] Teddy Lazebnik and Svetlana Bunimovich-Mendrazitsky. Generic approach for mathematical model of multi-strain pandemics. *PloS one*, 17(4):e0260683, 2022.
- [77] Viggo Andreasen, Jane Lin, and Simon A. Levin. The dynamics of cocirculating influenza strains conferring partial cross-immunity. *Journal of Mathematical Biology*, 35:825–842, 1997.

- [78] Julia R. Gog and Bryan T. Grenfell. Dynamics and selection of many-strain pathogens. *Proceedings of the National Academy of Sciences*, 99(26):17209–17214, 2002.
- [79] Pavlo Minayev and Neil M. Ferguson. Improving the realism of deterministic multi-strain models: implications for modelling influenza a. *Journal of the Royal Society Interface*, 6(35):509–518, 2009.
- [80] M. Gabriela M. Gomes, Lisa J. White, and Graham F. Medley. The reinfection threshold. *Journal of Theoretical Biology*, 236(1):111–113, 2005.
- [81] Amélia Nunes, M. Margarida Telo da Gama, and M. Gabriela M. Gomes. Localized contacts between hosts reduce pathogen diversity. *Journal of Theoretical Biology*, 241(2):477–487, 2006.
- [82] Martin Fudolig and Robert Howard. The local stability of a modified multi-strain sir model for emerging viral strains. *PLOS ONE*, 15(12):e0243408, 2020.
- [83] Laith J. Abu-Raddad and Neil M. Ferguson. The impact of cross-immunity, mutation and stochastic extinction on pathogen diversity. *Proceedings of the Royal Society of London. Series B: Biological Sciences*, 271(1556):2431–2438, 2004.
- [84] Isabel Gordo, M. Gabriela M. Gomes, D. G. Reis, and P. R. A. Campos. Genetic diversity in the sir model of pathogen evolution. *PLOS ONE*, 4(3):e4876, 2009.
- [85] Marie T. Meehan, Adam M. Rojek, Adegbeye I. Adekunle, Olumuyiwa A. Adegbeye, and Emma S. McBryde. Coupled, multi-strain epidemic models of mutating pathogens. *Mathematical Biosciences*, 296:1–17, 2018.
- [86] Teddy Lazebnik, Svetlana Bunimovich-Mendrazitsky, Shai Ashkenazi, Eugene Levner, and Arriel Benis. Early detection and control of the next epidemic wave using health communications: development of an artificial intelligence-based tool and its validation on covid-19 data from the us. *International Journal of Environmental Research and Public Health*, 19(23):16023, 2022.
- [87] Travis E Oliphant. Python for scientific computing. *Computing in science & engineering*, 9(3):10–20, 2007.
- [88] Svenska kyrkan. Svenska kyrkans medlemsutveckling år 1972–2024. PDF report, Svenska kyrkan i siffror (statistik), 2024. Accessed 2026-01-09.
- [89] Watch Tower Bible and Tract Society of Pennsylvania. 2024 service year report of jehovah’s witnesses worldwide. Web report, 2024.
- [90] Watch Tower Bible and Tract Society of Pennsylvania. 2024 country and territory reports. Web table (part of the 2024 Service Year Report), 2024.
- [91] Figure.NZ and Stats NZ. Census – usually resident population by religious affiliation, age group and region 2013, 2018 and 2023. Interactive table with download option, 2024.
- [92] Everett M. Rogers. *Diffusion of Innovations*. Free Press, New York, 5 edition, 2003.

- [93] Luigi Luca Cavalli-Sforza and Marcus W. Feldman. *Cultural Transmission and Evolution: A Quantitative Approach*. Princeton University Press, Princeton, NJ, 1981.
- [94] Robert Boyd and Peter J. Richerson. *Culture and the Evolutionary Process*. University of Chicago Press, Chicago, IL, 1985.
- [95] Damon Centola and Michael Macy. Complex contagions and the weakness of long ties. *American Journal of Sociology*, 113(3):702–734, 2007.
- [96] Laurence R. Iannaccone. The consequences of religious market structure: Adam smith and the economics of religion. *Rationality and Society*, 3(2):156–177, 1991.
- [97] Peter L. Berger. *The Sacred Canopy: Elements of a Sociological Theory of Religion*. Doubleday, Garden City, NY, 1967.
- [98] Pippa Norris and Ronald Inglehart. *Sacred and Secular: Religion and Politics Worldwide*. Cambridge University Press, Cambridge, UK, 2012.
- [99] D. J. Daley and D. G. Kendall. Stochastic rumours. *IMA Journal of Applied Mathematics*, 1(1):42–55, 1965.
- [100] KM Ariful Kabir, Kazuki Kuga, and Jun Tanimoto. Analysis of sir epidemic model with information spreading of awareness. *Chaos, Solitons & Fractals*, 119:118–125, 2019.
- [101] Laijun Zhao, Hongxin Cui, Xiaoyan Qiu, Xiaoli Wang, and Jiajia Wang. Sir rumor spreading model in the new media age. *Physica A: Statistical Mechanics and its Applications*, 392(4):995–1003, 2013.
- [102] Xiaobin Rui, Fanrong Meng, Zhixiao Wang, Guan Yuan, and Changjiang Du. Spir: The potential spreaders involved sir model for information diffusion in social networks. *Physica A: Statistical Mechanics and Its Applications*, 506:254–269, 2018.
- [103] QQ Zheng, JW Shen, V Pandey, YM Zhao, and LN Guan. Spatiotemporal dynamics of periodic waves in sir model with driving factors. *New Journal of Physics*, 25(6):063028, 2023.
- [104] Mateen Mahmood, André Victor Ribeiro Amaral, Jorge Mateu, and Paula Moraga. Modeling infectious disease dynamics: Integrating contact tracing-based stochastic compartment and spatio-temporal risk models. *Spatial Statistics*, 51:100691, 2022.
- [105] Thomas S Asbridge. *The first crusade: A new history*. Oxford University Press, 2004.
- [106] Ka U Ng. Are muslim immigrants assimilating? cultural assimilation trajectories in immigrants' attitudes toward gender roles in europe. *Journal of Ethnic and Migration Studies*, 48(15):3641–3667, 2022.
- [107] Charles M Macal. To agent-based simulation from system dynamics. In *Proceedings of the 2010 winter simulation conference*, pages 371–382. IEEE, 2010.
- [108] Pedro HT Schimit. Multi-strain epidemic models of mutating viruses with airborne transmission based on cellular automata and ordinary differential equations. *Axioms*, 12(7):632, 2023.

- [109] Anna Paula Galvão Scheidegger and Amarnath Banerjee. A comparison between a traditional seir-sei epidemiological model and a multi-strain, multi-vector disease spread model. In *IISE Annual Conference. Proceedings*, pages 2181–2186. Institute of Industrial and Systems Engineers (IISE), 2018.
- [110] Teddy Lazebnik and Avner Friedman. Comparing partial differential equations and agent-based simulations in spatio-temporal modeling of cancer growth and shape. *Journal of Computational and Applied Mathematics*, page 117183, 2025.

Appendix

Agent-based simulation driven model computing

Computation formalization

Due to the mutation mechanism, solving the ODE model over time is numerically challenging, as the number of equations is dynamic, which results in both discontinuous functions and high-dimensions [107, 108, 109]. As such, we decided to solve the proposed model using an agent-based simulation approach. Formally, each agent occupies exactly one state in $\{S, B_r, M_r, P_r : r \in \mathcal{R}\}$ with an associated religion label r (and $r = 0$ for S). The simulation evolves in discrete time steps of length Δt . Within each step, we apply stochastic transitions at the agent level using probabilities derived from the corresponding ODE rates via a hazard-to-probability mapping (e.g., $p = 1 - \exp(-\text{rate} \cdot \Delta t)$). This preserves non-negativity and implements the same mechanisms as the ODE in a finite population [110].

Within each step in time, we apply transitions using operator splitting: conversion/cross-conversion, role switching, disaffiliation, mutation, and demographic events are applied sequentially. Within each sub-step, at most one event of that type is applied per agent. Moreover, at time t , for each religion r we compute the force of conversion $\lambda_r(t) = \beta_r(t) M_r(t)/N(t)$ exactly as in the ODE. The ABS samples conversion events *per agent* using a total hazard, ensuring that each agent can undergo at most one conversion event per time step.

To this end, for an agent in S , the total conversion hazard is $h_S(t) = \sum_{k \in \mathcal{R}} \lambda_k(t)$, giving conversion probability $1 - \exp(-h_S(t)\Delta t)$. Conditional on conversion, the destination religion is sampled as r with probability $\lambda_r(t)/h_S(t)$, and the agent enters M_r with probability q_r or B_r with probability $1 - q_r$.

For an agent currently in B_r or M_r , the total cross-conversion hazard is $h_r(t) = \sum_{\ell \neq r} \lambda_\ell(t)$, with conversion probability $1 - \exp(-h_r(t)\Delta t)$. Conditional on conversion, the target religion $\ell \neq r$ is sampled proportionally to $\lambda_\ell(t)$, and the agent transitions to B_ℓ or M_ℓ according to q_ℓ . Priests P_r never switch religions and are excluded from conversion events.

Role switching is simulated via independent stochastic transitions: $B_r \rightarrow M_r$ at rate σ_r , $M_r \rightarrow B_r$ at rate κ_r , $B_r \rightarrow P_r$ at rate τ_r^B and $M_r \rightarrow P_r$ at rate τ_r^M . Disaffiliation is implemented as $B_r \rightarrow S$, $M_r \rightarrow S$, and $P_r \rightarrow S$ at rates ρ_r^B , ρ_r^M , and ρ_r^P , respectively. When an agent disaffiliates to S , its religion label is reset to $r = 0$.

Deaths are simulated in each compartment using the per-capita rate μ . Births are introduced using rate b while preserving the population composition in expectation: newborns are assigned to compartments proportionally to the current shares $X(t)/N(t)$, matching the ODE assumption of composition-preserving demographic turnover.

Mutation is applied only to missionaries. During each step, a missionary of religion r may relabel to a different religion ℓ (i.e., $M_r \rightarrow M_\ell$) with rate $\nu_{r\ell}$, meaning that mutation transfers missionaries between religions without

creating new agents; the role remains missionary while the religion label changes.

ODE-ABS compute comparison experiment design

In order to quantify the agreement between the ODE and the ABS implementation under the same parameterization, we compare the total-share time series $y_r^{\text{ODE}}(t)$ and $y_r^{\text{ABS}}(t)$ for each religion r , where $y_r(t)$ is defined as follows:

$$y_r(t) = \frac{B_r(t) + M_r(t) + P_r(t)}{N(t)}. \quad (12)$$

For ABS, we first average $y_r(t)$ across the R replicates and compute metrics on the replicate-mean series.

We report three standard time-series similarity measures: mean absolute error (MAE), root mean squared error (RMSE), and the coefficient of determination (R^2). Metrics are evaluated on a common time grid. For each parameterization (case), we compute metrics per religion and summarize overall agreement by taking unweighted arithmetic means across religions. Specifically, we generate $n_{\text{cases}} = 30$ parameterizations by taking Scenario A as a base configuration and applying independent multiplicative jitter to each parameter: $\theta \leftarrow \theta_{\text{base}} \cdot u$ and $u \sim \text{Uniform}(0.7, 1.3)$, for $\theta \in \{\beta_{r,0}, q_r, \sigma_r, \kappa_r, \tau_r^B, \tau_r^M, \rho_r^B, \rho_r^M, \rho_r^P\}$ (for each religion r). For the entry probability q_r , we clip the result to $[0, 1]$ after jittering. Mutation is enabled in the sweep: if a mutation matrix entry $\nu_{r,\ell}$ exists in the base configuration, it is also jittered multiplicatively by an independent factor in $[0.7, 1.3]$.

Demographic parameters (b, μ) , simulation controls $(\Delta t, T_{\text{max}})$, context flags/coefficients, and initial conditions are held fixed across the sweep. For each case, we solve the ODE once and run the ABS for $n = 20$ independent replicates, compute MAE/RMSE/ R^2 per religion on $y_r(t)$.

ODE-ABS compute comparison results

Fig. 5 presents the level of agreement in terms of both the coefficient of determination (R^2) and MAE between $n = 30$ cases computed in both ODE and ABS implementation. Notably, the cases are all without mutation in order to get an accurate evaluation of the ODE implementation. Overall, $R^2 = 0.974 \pm 0.021$ and $MAE = 0.0008 \pm 0.0005$ with a distribution of R^2 between 0.955 and 1.000 and MAE's between 0.00001 and 0.01800 which indicates a good agreement for both implementations.

Experiments settings

Table 1 summarizes the parameters used to generate the three cases presented in Fig. 2. These values are found manually using a trial-and-error approach.

Table ?? summarizes the parameters used to generate the three historical cases presented in Fig. 3. These values are found using data fitting procedure.

Fitting procedure

Given an observed affiliation time series $\{(t_i, y_{\text{obs}}(t_i))\}_{i=1}^n$, we map the data to a model observable $y(t) \in [0, 1]$ (the affiliated share for a focal religion/strain) and initialize at the first observation, $y(t_1) = y_{\text{obs}}(t_1)$. For computational efficiency, we calibrate a reduced 1-strain model that retains the two competing forces needed to reproduce

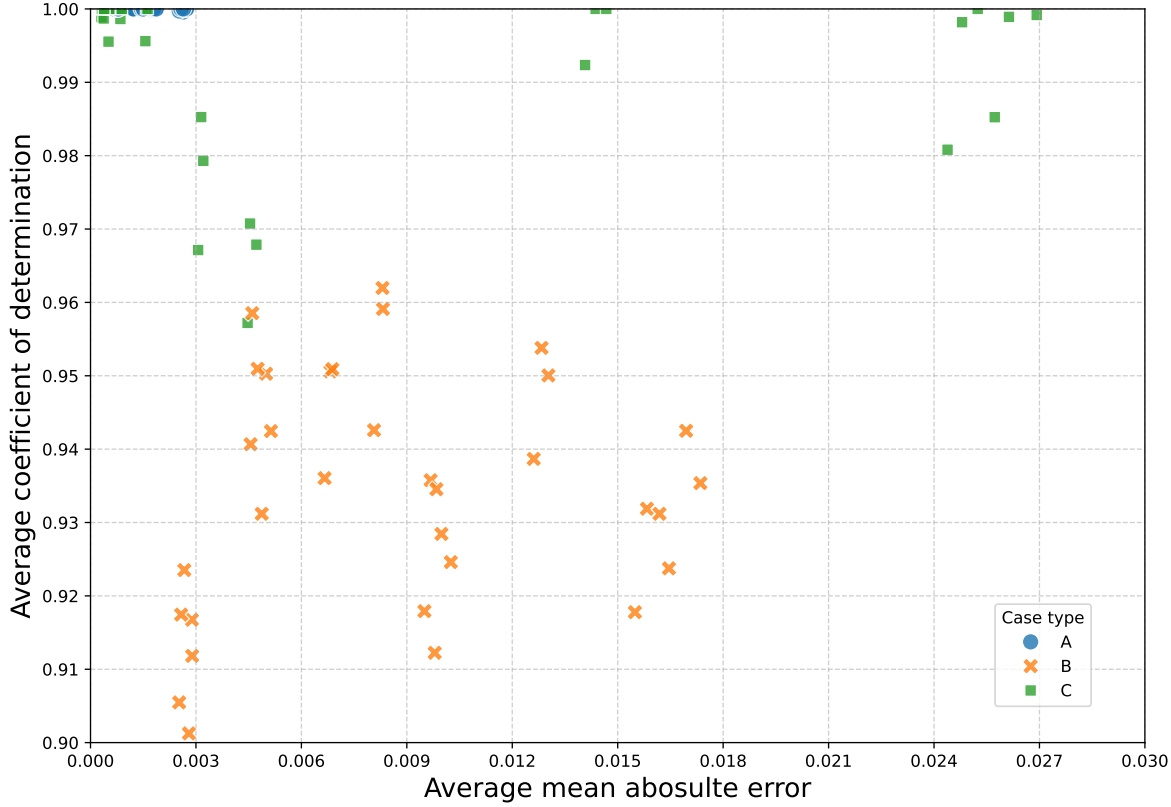


Figure 5: ODE-ABS agreement across $n = 99$ experiments with different parameter values over the three cases, like in Fig. ??, where each value i.

rise/decline in shares: recruitment from the complementary pool and disaffiliation,

$$\frac{dy}{dt} = \beta(t) y(t) (1 - y(t)) - \rho(t) y(t), \quad (13)$$

where $\beta(t)$ is an effective conversion/recruitment strength and $\rho(t)$ is an effective disaffiliation rate. Model trajectories are simulated in continuous time (adaptive Runge–Kutta; evaluated on a fine grid and sampled at the observation years), and parameters are estimated by minimizing the mean squared error

$$\text{loss} = \frac{1}{n} \sum_{i=1}^n (y_{\text{obs}}(t_i) - y_{\text{pred}}(t_i))^2$$

using box-constrained optimization (L-BFGS-B). To test whether nonstationary social conditions can be captured parsimoniously, we compare (i) a time-invariant baseline, $\beta(t) \equiv \beta$ and $\rho(t) \equiv \rho$, to (ii) a piecewise-constant variant with a fixed breakpoint t^* ,

$$\beta(t) = \beta_1 \mathbb{1}[t < t^*] + \beta_2 \mathbb{1}[t \geq t^*], \quad \rho(t) = \rho_1 \mathbb{1}[t < t^*] + \rho_2 \mathbb{1}[t \geq t^*],$$

which yields a minimal “regime-shift” hypothesis without introducing explicit exogenous covariates.

Parameter	Description	Scenario A	Scenario B	Scenario C
b	Birth rate	0.01	0.01	0.01
μ	Death rate	0.01	0.01	0.01
β_0	Baseline transmission	{1:0.03, 2:0.45}	{1:0.04, 2:0.02, 3:0.02, 4:0.02, 5:0.02, 6:0.02}	{1:0.28, 2:0.55}
q	Missionary fraction	{1:0.05, 2:0.1}	{1:0.05, 2:0.02, 3:0.02, 4:0.02, 5:0.02, 6:0.02}	{1:0.05, 2:0.05}
σ	$B \rightarrow M$ rate	{1:0.02, 2:0.03}	{1:0.02, 2:0.005, 3:0.005, 4:0.005, 5:0.005, 6:0.005}	{1:0.018, 2:0.018}
κ	$M \rightarrow B$ rate	{1:0.01, 2:0.01}	{1:0.02, 2:0.02, 3:0.02, 4:0.02, 5:0.02, 6:0.02}	{1:0.018, 2:0.018}
τ_B	$B \rightarrow P$ rate	{1:0.002, 2:0.003}	{1:0.002, 2:0.0003, 3:0.0003, 4:0.0003, 5:0.0003, 6:0.0003}	{1:0.0015, 2:0.0015}
τ_M	$M \rightarrow P$ rate	{1:0.003, 2:0.004}	{1:0.003, 2:0.0003, 3:0.0003, 4:0.0003, 5:0.0003, 6:0.0003}	{1:0.002, 2:0.002}
ρ_B	$B \rightarrow S$ (disaffiliation)	{1:0.005, 2:0.004}	{1:0.006, 2:0.05, 3:0.05, 4:0.05, 5:0.05, 6:0.05}	{1:0.006, 2:0.0225}
ρ_M	$M \rightarrow S$ (disaffiliation)	{1:0.004, 2:0.003}	{1:0.006, 2:0.15, 3:0.15, 4:0.15, 5:0.15, 6:0.15}	{1:0.006, 2:0.03}
ρ_P	$P \rightarrow S$ (disaffiliation)	{1:0.001, 2:0.001}	{1:0.001, 2:0.4, 3:0.4, 4:0.4, 5:0.4, 6:0.4}	{1:0.001, 2:0.003}
ν	Mutation rates	{1→2:0.002, 2→1:0}	{all:0}	{1→2:0, 2→1:0}

Table 1: Parameter settings for scenarios A, B, and C.

Model	β	ρ	K	Break year	y_0
Sweden (baseline)	1.00E-06	0.008095904			0.952
Sweden (piecewise)	0.1640045621058302 (pre)	0.021006932460500522 (pre)		2000	0.952
Turkey JW (baseline)	0.009874198824807388 (post)	0.025315477013951634 (post)	0.000120461		3.19E-05
Turkey JW (piecewise)	1000	0	0.000120461	2021	3.19E-05
New Zealand (baseline)	0.0 (pre)	0.0 (pre)			0.142663973
New Zealand (piecewise)	660.2129897320174 (post)	0.0 (post)		2013	0.142663973

Table 2: Historical fitting parameters.